Analysis and Simulation of Pile Driving Construction Equipment

Laszlo Kovacs[1], Eric Karpman[2], Marek Teichmann[1], Jozsef Kövecses[2]

[1]CM Labs Simulations, Montreal, Canada
[2]Dept. of Mechanical Engineering and Centre for Intelligent Machines
McGill University, Montreal, Canada

laszlo.kovacs@cm-labs.com, eric.karpman@mail.mcgill.ca

Abstract -

For real-time simulation of construction equipment, the operation of blades and other tools in contact with soil represent some of the most challenging problems both in terms of performance and accuracy. Soft soil interactions are particularly difficult to model and simulate efficiently, yet, a physically representative, interactive simulation that provides real-time feedback to the operator is required in operator training and certification scenarios, as well as for human in the loop engineering applications.
In this paper, we address the problem of simulating in real-time several piling techniques that are fundamental in construction. A sufficiently accurate resistance force/torque model is essential for the realistic simulation of piling equipment. Particle based models and finite element soil interaction models are too computationally expensive for most real-time simulations. We propose an analytical approach for estimating the piling resistance motivated by bearing capacity theories developed for deep foundations. The proposed model can accurately capture the soil resistance in three different piling scenarios: hammering, drilled displacement piling, and continuous flight augering. The vertical resistance force and torque, and their coupled nature is considered with kinetic friction effects. The presented models are validated against experimental data from subject matter experts. The results obtained for continuous flight augering are also compared to results from a discrete element simulation. To improve the realism of the analytical model, a hybrid numerical-analytical model is outlined. The proposed real-time models support fast equipment design iterations, control development, automation and interactive operator training.

Keywords -

real-time simulation. pile driving. soil-tool interaction. ground resistance. operator training.

1 Introduction

Using simulators to train operators of heavy construction site equipment requires the ability to efficiently model and simulate the interactions between tools and soil in an interactive and realistic way so that real time feedback can be provided to a human in the loop. In this work, our goal is to create a model of a drill rig that creates holes for foundation piles, an operation known as piling or pile driving. We propose a real-time model for three fundamental piling techniques used in the construction industry with a level of fidelity and realism that is appropriate for training drill rig operators. The three piling techniques of interest are the displacement pile with lost drill point, the continuous flight auger (CFA) and the hydrohammer.

The soil displacement piling operation with a lost drill point is an operation in which a large cylindrical pile with a conical tip is drilled into the ground by applying both a vertical force and a torque. Rather than removing soil from the ground, this operation displaces the soil downward and laterally. Once the pile has reached the desired depth, the pile is removed, leaving behind the drill point. The resulting hole is filled with concrete. Continuous flight augering is another excavation process in which the drill bit consists of a helical blade that removes the soil as it drills into the ground and a hollow shaft that is used to inject the concrete as the drill is removed.

Finally, the hydrohammer, or hydraulic impact hammer, is a tool that can be used to create holes for foundation piles through repeated hammering of a steel pile into the ground until the desired depth is reached. Fig. 1 illustrates the drilling tools used for each of these operations.

The Earthworks module in Vortex Studio [1], which is used for the models that will be described in this work, uses analytical formulas to estimate the cutting force resisting the motion of the tools interacting with the soil because these are efficient enough for real-time simulation. For the representation of the disturbed soil in motion, a particle based model is used.

In this paper, we present simple and efficient models

Figure 1. Displacement pile (top), continuous flight auger (middle) and hydrohammer (bottom) on a drill rig

to consider the force-torque coupling, and simulate the special case of cork-screwing. The model is based on classical bearing capacity formulas which we use in the context of dynamic simulation. We use data from industry experts as well as the results of DEM simulation to validate the qualitative and quantitative accuracy of the real-time model.

2 Theoretical Background

2.1 Soil-Tool Models

Soil can be modelled as continuum or by using particle representation for the individual grains. Both finite (FEM) and discrete element models (DEM) have limitations as the real soil is neither a continuum nor a collection of particles only. Water content may also play an important role as void ratio and pore pressure have an effect on the effective stress. The simulation of these models are also very computationally intensive. The Earthworks module in Vortex therefore uses analytical formulas to estimate the cutting force resisting the motion of the tools interacting with the soil, while for the representation of the disturbed soil in motion a particle based model was developed. The cutting force estimation is based on the fundamental earth-moving equation (FEE) [2]. In situations, where the visual representation of the cut and the effect of the transported soil is not important, applying purely analytical models could be sufficient. This is the case when a drill rig is creating holes for foundation piles at a relatively slow penetration rate.

The model behind the FEE equation is two dimensional, i.e., the cutting tool is considered to have an infinite width. Another common assumption is that the soil fails along a straight line starting at the tip of the tool and reaching the soil surface at a distance ahead of the tool. The tool is a flat blade and the slope of the failure line depends on the internal friction angle of the soil. The soil resistance is approximated based on the quasi-static equilibrium of the soil wedge formed in front of the blade. By assuming passive soil failure, Rankine's passive earth pressure theory and the Mohr-Coulomb failure criterion can give an approximate value for the soil wedge angle which is valid for frictionless, vertical blades with a flat soil surface [3]. The soil wedge angle can also be estimated by minimizing the weight related N-factor in the FEE [4]. In Luengo's work [5], the soil-tool interaction was studied in an automated excavation scenario, where the FEE was modified to also include the effect of the slope of the terrain.

Similar models were developed to assess the bearing capacity of foundations. For shallow strip foundations Therzaghi's bearing capacity formula [6] can be used. To account for deviations from shallow strip foundations, several different bearing capacity and correction factors exist [7, 8, 9, 10]. Empirical shape factors are used to consider the actual shape (e.g., circular cross-subsection) of the pile. Several authors proposed similar formulas by considering installation depth and inclination. In soil augering and robotic drilling the soil/material moved by the flights of the auger and transported to the surface has an important effect on the resistance felt by the tool. In case of augering the flights are typically full of compacted soil and the soil-tool interaction is simultaneous on all the surfaces of the auger and the borehole. In case of drilling, separate particles are being transported, the motion of which also depend on the centrifugal effects at higher rotation speeds [11]. A special operation which can happen in case of soil augering is called cork-screwing. In this case the downward velocity is such that the penetration in one turn is equal to the pitch and the uplift velocity of the soil is zero. The drill screws into the soil as the worm of a corkscrew.

Compared to the cutting force resistance model, the estimation of the ground reaction for piles and drill bits are more complicated in the sense that the reaction force/torque has more components, and there is coupling between the reaction force and torque. When rotary displacement piles are pulled into the ground by the drill rig, the cylindrical surface of the pile comes into contact with the soil, and, in addition to the tip resistance, a depth dependent and distributed friction force develops along the embedded length of the pile. As the pile rotates, the direction of the resultant friction force changes with the instan-

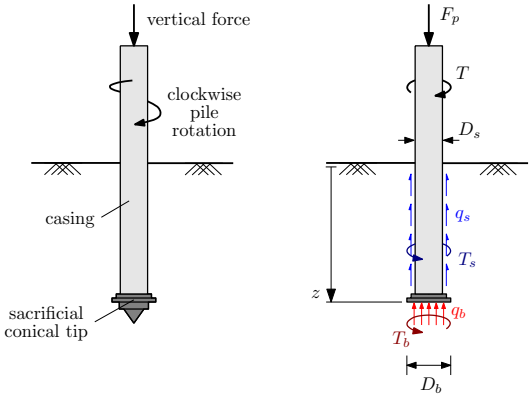

Figure 2. Loading and reactions of circular cross subsection pile

taneous pitch of the pile. At high rotational speeds with slow penetration this generates a large resistance torque, whereas at a low rotation rate the vertical component of the friction force will dominate. This phenomenon is used to lower the skin resistance below certain depths to reduce the necessary piling force.

2.2 Ground Resistance Force

When a pile is already installed in the ground, two main resistance force components can be distinguished. These are the base or tip resistance and the skin resistance. The base resistance is a localized property whereas the skin resistance, which depend on the embedded surface area of the pile, depend on the composition of the soil layers.

Due to the complexity of the problem, piles are often designed using empirical methods. This is based on on-site measurements, i.e., the bearing capacity of the pile is correlated with cone penetrometer test data. Another approach for estimating the resistance is to use analytical models that are based on certain failure criteria of the soil. An advantage of these analytical models is that they depend on a relatively limited number of parameters and can provide a tunable model for simulation. In case of the ground model developed for the IHC project the latter approach was followed.

Pile design formulas are valid under the assumption that the pile is advancing slowly and a quasi-static model is applicable. The formulas presented below are based on this assumption. Additional kinematic considerations were necessary to model the resistance of the different piles. Under slow rotation and penetration, the main ground reaction components are presented in Fig. 2, where F_p and T are the applied piling force and torque, q_b and q_s are the distributed base and skin reaction forces, and T_b and T_s are the resultant base and skin resistant torques.

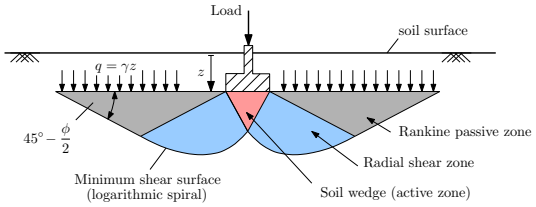

Figure 3. Assumed soil failure in case of shallow strip foundations

2.2.1 Base resistance

The resistance of the soil at the tip of the pile is often calculated by using Therzagi's bearing capacity formula [6]. This is valid for strip foundations at a shallow depth, but empirical shape factors are used to consider the actual shape (e.g., circular cross-subsection) of the pile. Terzaghi's assumption for shallow strip foundations is shown in Fig. 3. In this figure, z denotes the depth of the tip of the pile, γ is the specific weight of the soil, and ϕ its internal friction angle. In addition, q denotes the overburden pressure due to the weight of the soil. There are three distinct zones identified, and the soil is assumed to fail (be able to slide) along the edges of these zones. The bearing capacity of the soil can be calculated by analyzing the static equilibrium of the soil wedge shown below the pile.

The ultimate bearing capacity of foundations has the general form [7]:

$$q_b = c\, d_c S_c N_c + \gamma z\, d_q S_q N_q + 0.5 \gamma d_\gamma\, S_\gamma N_\gamma \quad (1)$$

where c, $q = \gamma z$ and γ are the cohesion, overburden pressure and specific weight of the soil, and N_c, N_q and N_γ are the corresponding bearing capacity factors. These factors have an intricate dependence on the internal friction angle of the soil. In addition, d_* and S_* denote different depth and shape factors that are used to adjust the contribution of the additive terms. The resulting base resistance pressure q_b can be used to estimate the resistance of the ground during piling as the force $Q_b = q_b A_b$ represent the limit force (bearing capacity) at which the pile should sink into the ground, where A_b is the area of the base of the pile.

According to Terzaghi [6], the bearing capacity factors are

$$\begin{aligned} N_q &= \frac{e^{2(3\pi/4-\phi/2)} \tan(\phi)}{2\cos(\pi/4+\phi/2)^2} \\ N_c &= \frac{N_q - 1}{\tan(\phi)} \\ N_\gamma &= \frac{\tan(\phi)}{\gamma}\left(\frac{K_{p\gamma}}{\cos(\phi)^2} - 1\right) \end{aligned} \quad (2)$$

where $K_{p\gamma}$ is the passive soil pressure coefficient usually given in the form of tabulated data in the function of the internal friction angle. A simpler form of the last bearing

capacity factor above was proposed by Coduto [12]:

$$N_\gamma = \frac{2(N_q + 1)\tan(\phi)}{1 + 0.4\sin(4\phi)} \tag{3}$$

The shape and depth factors in Eq. (1) for circular footing are

$$S_q = 1, \quad S_c = 1.3, \quad S_\gamma = 0.6 \quad \text{and} \quad d_q = d_c = d_\gamma = 1 \tag{4}$$

Considering deep foundations, and therefore different soil failure lines, Meyerhof proposed different bearing capacity factors [7] :

$$\begin{aligned} N_q &= \mathrm{e}^{\pi\tan(\phi)}\tan(\pi/4 + \phi/2)^2 \\ N_c &= \frac{N_q - 1}{\tan(\phi)} \\ N_\gamma &= (N_q - 1)\tan(1.4\phi) \end{aligned} \tag{5}$$

where the shape and depth factors are:

$$\begin{aligned} S_q &= 1 + 0.1K_p, \\ S_c &= 1 + 0.2K_p, \\ S_\gamma &= S_q \end{aligned} \tag{6}$$

with

$$\begin{aligned} K_p &= \tan(\pi/4 + \phi/2)^2 \\ d_q &= 1 + 0.1\sqrt{K_p}, \quad d_c = 1 + 0.2\sqrt{K_p}, \quad d_\gamma = d_q \end{aligned} \tag{7}$$

A more recent study by van Baars [10] proposes another expressions for the shape factors. These are:

$$\begin{aligned} S_q &= 1 + 1.5\sin(\phi) + 3\tan(\phi)^3\,, \\ S_c &= S_q + (0.2 - 0.1\tan(\phi))\,, \\ S_\gamma &= S_q \end{aligned} \tag{8}$$

It can be seen that the bearing capacity factors N_c and N_γ are typically expressed with the help of N_q. Therefore, in Fig. 4 the tip resistances obtained by different authors are presented by comparing this bearing capacity factor. By noticing the logarithmic scale of the vertical axis, it is clear that there are very significant difference between the models that are available in the literature, but at the same time, they are qualitatively similar.

During pile driving, the base resistance provided by these formulas can significantly drop due to the disturbance of the soil when the pile rotates. On the other hand, when the penetration speed is suddenly increased, the soil might temporarily have a higher resistance as the stresses around the tip of the pile does not have time to relax.

Assuming a constant base resistance, and a corresponding constant linear shear stress distribution under the tip of the pile, the base resistance force and torque can be expressed as:

$$Q_b = \frac{D_b\pi^2}{4} q_b \quad \text{and} \tag{9}$$

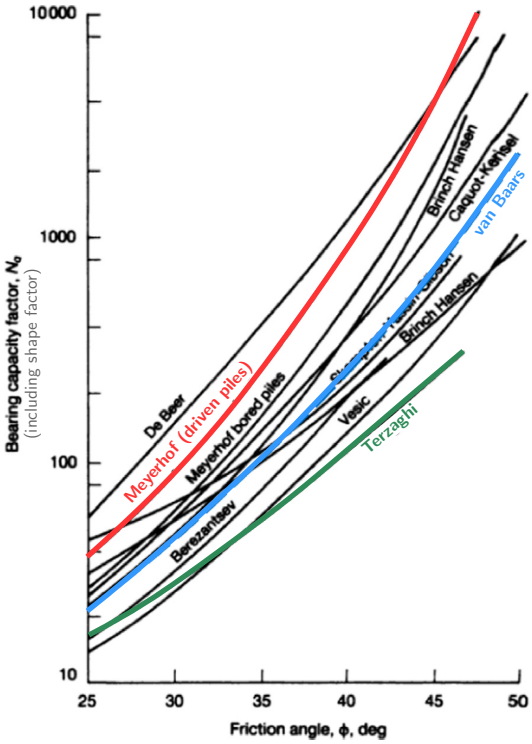

Figure 4. Different bearing capacity factors [10]

$$T_b = \int_0^{D_b/2} (\tan(\delta)\, q_b\, 2r\pi\, r)\ \mathrm{d}r = \tan(\delta)\, Q_b \frac{D_b}{3} \tag{10}$$

where δ is the friction angle between the soil and the pile's material and D_b is the diameter of the sacrificial tip.

2.2.2 Skin resistance

The skin resistance of piles is a frictional resistance force which depends on the pressure exerted by the soil on the surface of the pile. This lateral earth pressure is proportional to the overburden pressure, and changes significantly with the state of the soil. The active surface area also depend on embedded depth of the pile, so the depth dependence of the skin resistance is quadratic. When this resistance is calculated the composition of the soil layers has to be considered too. The total skin resistance force is the force which is acting on the complete embedded surface of the pile.

The lateral soil pressure is proportional to the overburden pressure. There are different theories to estimate the ratio between these. In case when the soil is undisturbed, the so-called in-situ soil pressure coefficient, K_0, can be calculated by using Jaky's simplified formula [13]. When the soil can expand and the stresses can relax, it is said to be active and the lateral pressure, K_a, is smaller than the in-situ pressure. When the soil is compressed (e.g.,

displaced by the pile) it is said to be passive and the lateral pressure, K_p, is significantly higher. The active and passive soil pressures are often estimated based on Rankine's theory. For cohesionless soils:

$$K_0 = 1-\sin(\phi), \quad K_a = \frac{1-\sin(\phi)}{1+\sin(\phi)}, \quad K_p = 1/K_a \quad (11)$$

In the pile design literature, various different formulas and tabulated experimental results exist for determining the lateral earth pressure coefficient, K, that can be used for the skin resistance calculation based on the piling technique and the specific soil type. Empirical factors are necessary to accompany the pure soil mechanics formulations to consider all the effects that can change the bearing capacity of a pile after it is inserted [14]. Recommendations for choosing the proper earth pressure coefficient, including averaging the formulae in Eq. (11), were proposed by Wrana [15]. For simulating the insertion process of a driven displacement pile in an operator training scenario, a good default value could be $K = K_p$ and introducing an additional scaling factor could allow the user to fine tune the soil behaviour. With these consideration the skin resistance force can be calculated as the integral:

$$Q_s(z) = \int_0^z (\tan(\delta) K q D_s \pi)\ \mathrm{d}\zeta \quad (12)$$

where the overburden pressure q, the lateral earth pressure coefficient K, and the friction coefficient $\tan(\delta)$ depend on the soil depth and the composition of soil layers. With the assumption of having constant soil properties per layer, this integral can be pre-computed in closed form for the real time simulation, or a simple 1 dimensional lookup table (with linear interpolation) can be used to quickly obtain the skin resistance force at specific depths. In order to incorporate the effect of pile rotation on the skin resistance, the instantaneous pitch of a rotary displacement pile needs to be considered. As the pile rotates, a point on it's surface moves relative to the ground with the sum of the tangential and axial velocities. The skin friction opposes this resultant velocity. The decomposition of the friction force into a radial and an axial component helps understanding, and captures the important effect, that in practice the rotation of a pile makes its insertion easier at the expense of increasing the overall resistance torque. The reduced skin resistance (the vertical component of the friction force) and the resistance torque which increases with the rotation speed can be computed in the form:

$$Q_{sv} = Q_s \frac{v_a + v_{min}}{v + v_{min}} \quad \text{with} \quad v = \sqrt{v_a^2 + v_t^2} \quad (13)$$

$$T_s = R_s Q_s \frac{v_t + v_{min}}{v + v_{min}} \quad (14)$$

where v_a is the axial velocity, $v_t = R_s\omega$ is the tangential velocity with radius R_s, and ω is the angular velocity of the pile. The minimum velocity v_{min} parameter was introduced to handle the special cases during simulation when one or both of the velocity components are zero. In case of the latter, when the pile is not moving, $Q_{sv} = Q_s$ and $T_s = R_s Q_s$ represent the maximum force and torque bounds of the constraints modelling the reaction torque and force, respectively.

3 Real Time Soil Augering Model

In our real time simulation model, we consider 4 different generalized reaction forces. These are the extraction and penetration resistance forces, the resistance torque and the pull-down force exerted by the auger on the piling equipment. The main characteristics of these are captured by simple models that provide an efficient formulation and qualitatively accurate results. During extraction, it is assumed that the auger does not rotate, and the weight of the pile is calculated considering the flights of the auger are completely filled with soil. In this case the extraction resistance force can simply be calculated by using the skin resistance force derived in the previous section plus the weight of the soil. For the skin resistance computation, one can simply use the borehole diameter as the skin diameter (D_s) and replace the external (soil-pile) friction angle (δ) with the internal friction angle (ϕ) of the soil.

For estimating the penetration resistance force, three different operation regimes can be considered. First, when the auger is rotating relatively fast and it is transporting soil to the surface. Second, when the instantaneous pitch is equal to pitch of the helix of the auger, and the auger is corkscrewing itself into the ground with a rapidly increasing resistance torque. And third, when the linear downward motion dominates and the auger displaces soil similar to a displacement pile. In this third case, the estimation of the penetration resistance is relatively simple as it ends up being the skin resistance calculated with the borehole diameter and the internal friction angle of the soil. When soil is transported or corkscrewing happens further considerations are necessary.

The helix of the auger can be seen as a long wedge along which the total mass of the soil is pushed upwards. The uplifting force is the resultant of force transmitted from the helix to the soil minus the resistance force due to friction with the wall of the borehole. In order to estimate these forces, the kinematic model in Figure 5 is considered. This shows that the $\vec{v}_{\text{up}}$ uplifting transport velocity of the soil is the sum of the auger's downward velocity $v_z\,\hat{k}$, the lateral velocity $\vec{v}_t = r\omega\,\hat{t}$ and the relative soil velocity with respect to the auger $\vec{v}_{\text{rel}}$. The magnitude of the uplifting velocity ranges from zero to $v_{\text{up,max}} = v_t\tan(\psi) - v_a$ where $v_a = -v_z$ is the penetration velocity. In the following, this maximum velocity is used to express the uplifting velocity $v_{\text{up}} = \eta\, v_{\text{up,max}}$ where η is an efficiency parameter. It is left to the user to define this as a constant, or feed back

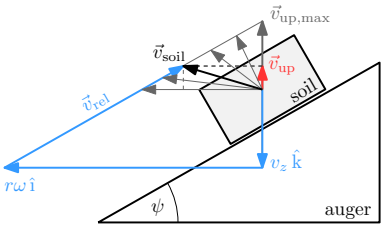

Figure 5. Model of soil uplift velocity of the auger

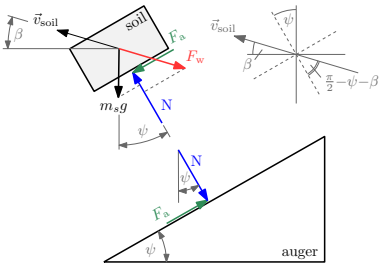

Figure 6. Free body diagram of the augering model

its value to the model using complementary calculations. With these considerations, the penetration resistance (Q_a) and the pull-down force (V_a) of the aguer can be expressed by using the free body diagrams shown in Figure 6 as

$$Q_a = F_a \sin(\psi) \tag{15}$$

$$V_a = N \cos(\psi) \tag{16}$$

with

$$N = m_s g \cos(\psi) + F_w \sin(\psi + \beta) \tag{17}$$

$$F_a = \tan(\delta) N \tag{18}$$

where N and F_a are the normal and lateral components of the reaction force between the soil and the auger. The total mass of the soil is m_s, g is the gravitational acceleration, and F_w is the total skin resistance force transmitted from borehole to the soil mass in the auger. Moreover, using the outer radius r of the auger, an upper bound on the augering resistance torque can be given in the form:

$$T_s = (F_a \cos(\psi) + N \sin(\psi))\, r \tag{19}$$

In the special case when the maximum uplifting velocity $v_{\text{up,max}}$ is zero, the auger is corkscrewing. This condition is identical to saying that the instantaneous pitch $v_a/v_t = \tan\psi = p/(2\pi)$ with p being the pitch (height difference) between the flights of the auger. When this happens the auger is pulling itself into the ground as a corkscrew into the cork, and the reaction force and torque increase until the machine limits are reached and the auger cannot be moved further into the soil. This dangerous situation must be avoided, and a trained operator needs to change the penetration and rotation speed in order to prevent this from happening. For such a training, we use a model, where a kinematic constraint is used to lock

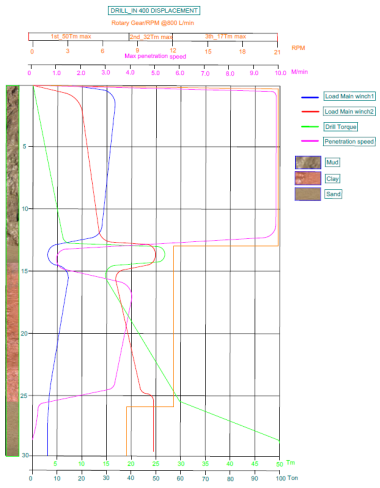

Figure 7. IHC reference data for displacement drill

the auger into the corkscrewing regime, with rapidly increasing reaction force and torque, when the instantaneous pitch is sufficiently close to geometric pitch (expressed in m/rad) of the auger. The maximum force and torque of this screw constraint is proportional to the corkscrewed length of the auger. This way, when the user sufficiently unscrews the auger the applied torque and force can overcome the constraint limits, and the auger can break out of corkscrewing.

4 Model Validation

The IHC FUNDEX F3500 multifunctional foundation rig was modelled and simulated. The main objective was to develop real-time, parametric and physically motivated ground resistance models for three different pile driving operations. These include the displacement drill, the continuous flight auger (CFA) and the hydrohammer piling techniques. In each case, the pile is driven into the ground by the drill rig and it penetrates through different layers of soil with different resistances. As the programmable logic controller (PLC) of the simulated drill rig is integrated into the system, it expects to receive physically realistic resistances. Therefore, selection and tuning of soil properties was an important element of the work.

For the validation of the model, IHC industry experts provided us with desired drill report curves. Figure 7 shows an example of the provided report for the expected soil resistance during displacement drilling. The desired behaviour was determined based on real drill reports by capturing the main characteristics of experimentally recorded data. The report shows vertical force and torque applied to the tool, as well as the penetration and angular velocities of the tool. There are three distinct soil layers that the tool passes through as depth increases: mud, clay, and sand.Capturing the effect of layer transitions is

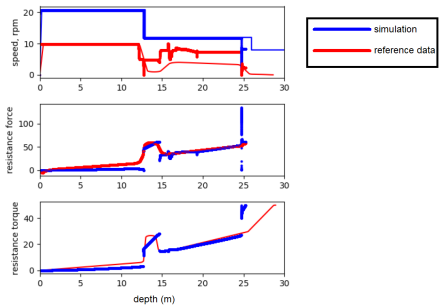

Figure 8. Machine in the loop simulation results

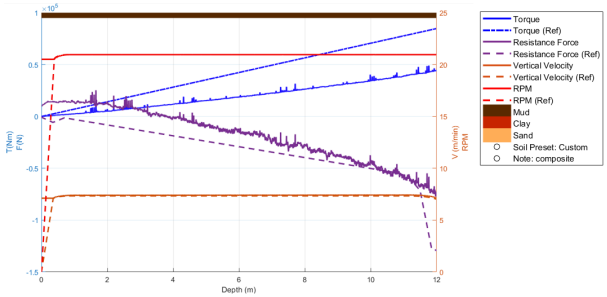

Figure 9. DEM Simulation results - CFA

an important aspect of the simulation. The reason we did not directly use some recorded drill reports is that in the simulated scenario there were only four layers with very different soil properties. The four layers and the composition of the layers can be chosen by the instructor of the training simulator according to the pedagogical needs.

In Fig. 8 the drill report of a displacement drill operation is shown. In the top panel the thin lines represent the planned penetration rate (speed) and rotation speed (rpm), and the thicker lines show the actual values commanded by the operator of the simulator. These are plotted as function of the penetration of the tip of the pile (not wrt. time). The middle panel depicts the observed (blue) resistance force vs. the expected one (red). Similarly, the comparison of the resistance torques can be seen in the bottom panel. Although, the penetration speed was generally slower than the desired value, the soil resistance matches the expected trends and values quite closely. Note, the equations used to estimate the ground reaction assume quasi-static conditions, therefore they cannot directly capture the effect of different penetration speeds.

5 DEM Model

Because DEM has a well documented ability to produce high-fidelity soil models [16], a DEM simulations was set up to show that the purely analytical model, as well as the reference data, was qualitatively in agreement with a DEM approach. In this section, we present the comparison for the CFA simulation using DEM.

The DEM model of the drill rig was built in the real time multibody simulation platform Vortex Studio [1] whose particle system is based on the Parallel Particles approach to DEM modelling proposed by Holz [17], based on the principles of position-based dynamics presented by Muller [18]. This method has previously been used for DEM soil simulations of wheels travelling over soil [19] [20] and blades excavating soil [20]. Due to current software limitations, the DEM simulations only consider the behaviour of the drill for the first 12 meters depth, at which point the reference data indicates a transition from the mud soil layer to clay. This is because the current version of this DEM implementation does not make it possible to model layers of soil with different properties. However, conclusions can still be drawn from the simulation of the first soil layer, which accounts for about a third of the total depth included in the IHC reference data.

Figure 9 shows a comparison between the reference data that was used in the previous section and the DEM simulation results for the continuous flight auger. Extensive tuning would be required in order to achieve a perfect quantitative match with the DEM simulation [19], but the simulation results with baseline soft soil parameters already showed good qualitative agreement. Without tuning of parameters, we are looking for the DEM model to replicate the overall trend of the outputs as depth increases, as well as the order of magnitude of the outputs. The doted lines on the plot show the reference values for torque, resistance force, penetration speed and RPM; while the solid lines show the results of the DEM simulation. Unlike the analytical model, this DEM model is a fully dynamic rigid body simulation coupled with a particles to model the soil. Velocity level constraints control the motion of the drill, allowing the simulation to exactly match the desired motion of the drill - illustrated in red and orange for the RPM and vertical velocity, respectively. In the interest of simulation time, the particles used in the simulation were rather coarse, which explains the noisy nature of the resistance force and torque outputs. While the order of magnitude and overall trend with respect to depth of the force and torque plots are consistent with the reference data, the inaccuracy of the exact numerical value of these outputs can be attributed to a lack of parameter tuning.

6 Conclusion

This paper proposes an analytical method for modelling piling operations for real time dynamic simulation which is accurate and efficient enough for the purposes of operator training. The model uses classical bearing capacity equations to compute the force components acting on the pile during insertion. To capture the reduction of the vertical resistance force when the pile is rotated, a simple

model was developed to decompose the overall friction force based on the instantaneous pitch. This is essential for building a realistic scenario for operator training when a rotary displacement pile is used.

Another important contribution of the paper is the simplified augering model that was presented. This model simulates the vertical pull down force of an auger reasonably well. The selected semi-analytical simulation approach was necessary to achieve the simulation speed and accuracy required for successful operator training. It enables real time training with PLC in the loop. This model is dependent on proper tuning of an efficiency parameter for the uplifting force that is left to the user to define, either as a constant value or through some complementary calculations. Setting this value as a constant and tuning it, the qualitative agreement between the presented models is realistic enough for human-in-the-loop drill operator training simulators. This claim was validated by comparing the analytical results to reference data provided by industry experts - data that was in turn qualitatively compared to a dynamic discrete element soil model for the first layer of soil.

References

[1] CM Labs Simulations. Vortex studio simulation platform, 2018. URL https://www.cm-labs.com/vortex-studio/.

[2] A.R. Reece. Paper 2: The fundamental equation of earth-moving mechanics. Proceedings of the Institution of Mechanical Engineers, 179(6):16–22, June 1, 1964.

[3] V.N.S Murthy. Geotechnical engineering: Principles and practices of soil mechanics and foundation engineering. CRC Press, Boca Raton, FL, 2002.

[4] Fiorenzo Malaguti. Soil machine interaction in digging and earthmoving automation. 12 1994. doi:10.1016/B978-0-444-82044-0.50029-1.

[5] O. Luengo. Modeling and identification of soil-tool interaction in automated excavation. In Proceedings of the IEEE/RSJ International Conference on Intelligent Robotic Systems, page 7 pages, Victoria, BC, Canada, October 13-17, 1998.

[6] K. Terzaghi. Theoretical Soil Mechanics. Wiley, New York, 1943.

[7] G.G. Meyerhof. The ultimate bearing capacity of fundations. Geothecnique, 2(4):301–331, 1951.

[8] G.G. Meyerhof. Some recent research on the bearing capacity of foundations. Canadian Geotechnical Journal, 1(1):16–26, 1963.

[9] J.B. Hansen. A revised and extended formula for bearing capacity. In Bulletin No. 28, pages 5–11. The Danish Geotechnical Insititue, Copenhagen, 1970.

[10] S. van Baars. The inclination and shape factors for the bearing capacity of footings. Soils and Foundations, 54(5):985–992, 2014.

[11] Quan Qiquan, Tang Junyue, Yuan Fengpei, Jiang Shengyuan, and Deng Zongquan. Drilling load modeling and validation based on the filling rate of auger flute in planetary sampling. Chinese Journal of Aeronautics, 30(1):434–446, 2017.

[12] D. Coduto. Foundation Design. Prentice-Hall, 2001.

[13] J. Jaky. Pressure in silos. In Proceedings of the second international conference on soil mechanics and foundation engineering, pages 103–107, Rotterdam, June 21–30, 1948.

[14] Michael Tomlinson and John Woodward. Pile Design and Construction Practice. CRC Press, Boca Raton, FL, 6 edition, 2015.

[15] Bogumil Wrana. Pile load capacity – calculation methods. Studia Geotechnica et Mechanica, 37(4), 2015.

[16] William Smith, Daniel Melanz, Carmine Senatore, Karl Iagnemma, and Huei Peng. Comparison of discrete element method and traditional modeling methods for steady-state wheel-terrain interaction of small vehicles. Journal of Terramechanics, 56:61–75, 2014.

[17] D. Holz. Parallel particles (p2): A parallel position based approach for fast and stable simulation of granular materials. Workshop on Virtual Reality Interaction and Physical Simulation VRIPHYS, 2014.

[18] M. Muller, B. Heidelberger, M. Hennix, and J. Ratcliff. Position based dynamics. Journal of Engineering Mechanics, 2006.

[19] Eric Karpman, Jozsef Kovecses, Daniel Holz, and Krzysztof Skonieczny. Discrete element modelling for wheel-soil interaction and the analysis of the effect of gravity. Journal of Terramechanics, 91:139–153, 2020.

[20] Eric Karpman, Jozsef Kovecses, and Marek Teichmann. Terramechanics models augmented by machine learning representations. Journal of Terramechanics, 107:75–89, 2023.